Supporting Information

CHEF induced highly selective and sensitive turn-on fluorometric and colorimetric sensor for Fe^{3+}

Shyamaprosad Goswami,[*a] Sangita Das,[a] Krishnendu Aich,[a] Deblina Sarkar,[b] Tapan Kumar Mondal,[b] Ching Kheng Quah[c] and Hoong-Kun Fun[c,d]

[a]*Department of Chemistry, Bengal Engineering and Science University, Shibpur, Howrah, INDIA, 711 103, Tel. +91-33-2668 4561-3 ext. 498; Fax. +91-33-2668 2916.*

E-mail spgoswamical@yahoo.com

[b]*Department of Chemistry, Jadavpur University, Kolkata- 700032, India*

[c] *X–ray Crystallography Unit, School of Physics, Universiti Sains Malaysia, 11800 USM, Penang, Malaysia.*
[d]*Department of Pharmaceutical Chemistry, College of Pharmacy, King Saud University, Riyadh 11451, Saudi Arabia; E-mail: hfun.c@ksu.edu.sa*
Tel Office : (+966) 146-77335 Fax : (+966)146-76220

CONTENTS

General method of UV-vis and fluorescence titration:

By UV-vis method

Binding constant was calculated according to the Benesi-Hildebrand equation. *Ka* was calculated following the equation stated below.

$$1/(A\text{-}Ao) = 1/\{K(A_{max}–Ao)\ [M^{x+}]^n\} + 1/[A_{max}\text{-}A_o]$$

Here Ao is the absorbance of receptor in the absence of guest, A is the absorbance recorded in the presence of added guest, A_{max} is absorbance in presence of added $[M^{x+}]_{max}$ and K is the association constant. The association constant (K) could be determined from the slope of the straight line of the plot of $1/(A\text{-}Ao)$ against $1/[M^{x+}]$ and is found to be $1.04 \times 10^4\ M^{-1}$.

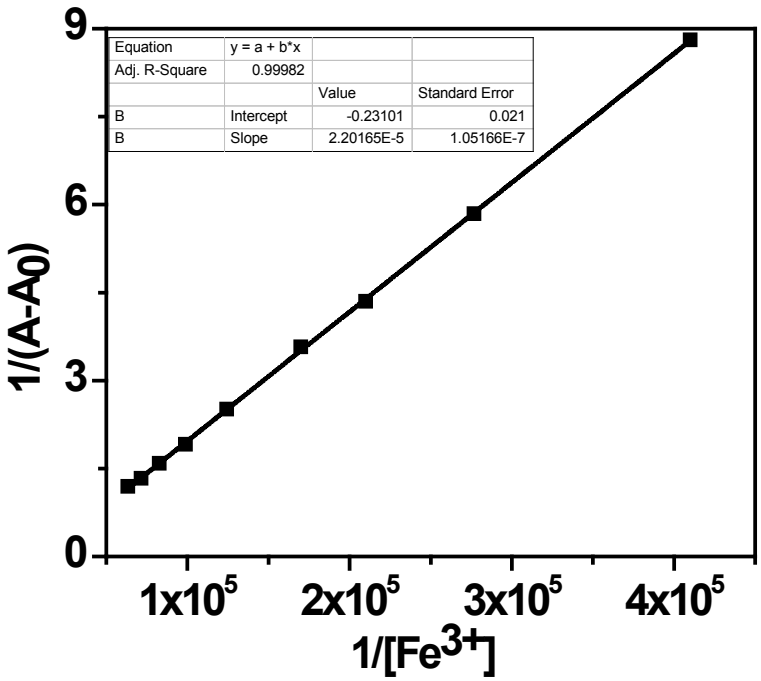

Figure S1: Benesi-Hildebrand plot from absorption titration data of receptor (20 μM) with Fe^{3+}.

General procedure for drawing Job plot by UV–vis method

Stock solution of same concentration of the receptors and the guest were prepared in the order of ca. 2.0 x 10^{-5} ML^{-1} CH_3CN-H_2O (1:1, *v/v*). The absorbance in each case with different *host–guest* ratio but equal in volume was recorded. Job plots were drawn by plotting $\Delta I.X_{host}$ *vs* X_{host} (ΔI = change of intensity of the absorbance spectrum during titration and X_{host} is the mole fraction of the host in each case, respectively).

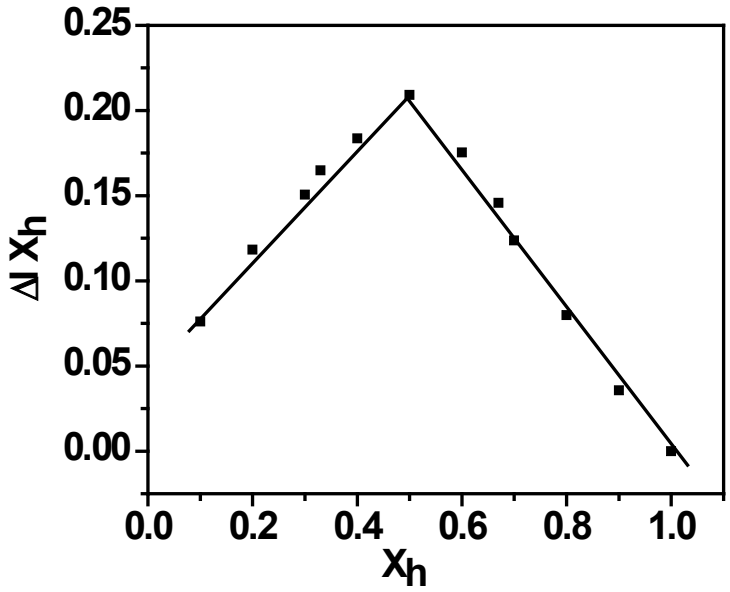

Figure S2: Job's plot diagram of receptor for Fe^{3+} ion (where X_h is the mole fraction of the host and ΔI indicates the change of absorbance at 530 nm).

By fluorescence method:

The binding constant value of Fe^{3+} with receptor has been determined from the emission intensity data following the modified Benesi–Hildebrand equation, $1//\Delta I = 1//\Delta I$ max $+(1/K[C])(1//\Delta I$ max). Here ΔI = I-Imin and ΔI max = Imax-Imin, where Imin, I, and Imax are the emission intensities of receptor considered in the absence of Fe^{3+}, at an intermediate Fe^{3+} concentration, and at a concentration of complete saturation where K is the binding constant and [C] is the Fe^{3+}concentration respectively. From the plot of [1 / (I_{min} –I)] against $[C]^{-1}$ for receptor, the value of K has been determined from the slope. The association constant (K_a) as

determined by fluorescence titration method for the receptor with Fe^{3+} is found to be 5.9×10^5 M^{-1} (error < 10%).

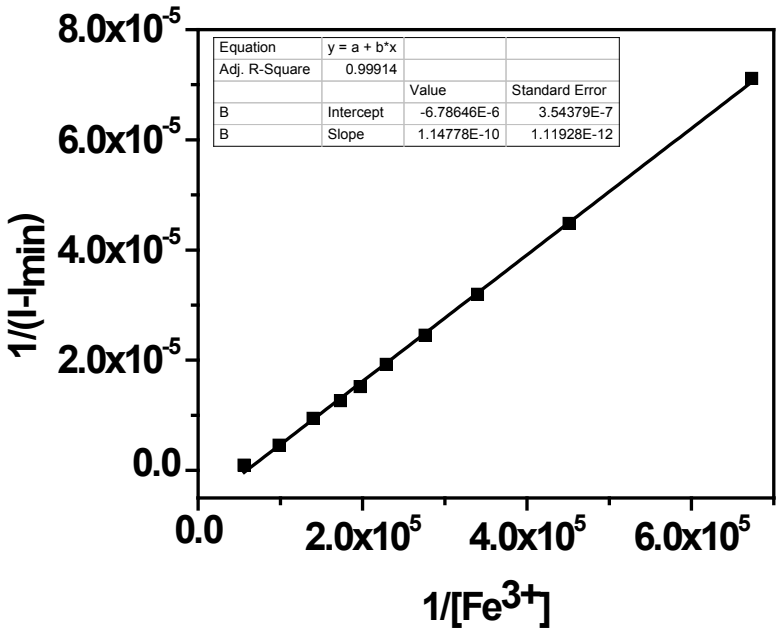

Figure S3: Benesi–Hildebrand plot from fluorescence titration data of receptor (2 μM) with Fe^{3+}.

Determination of detection limit:

The detection limit was calculated based on the absorption and fluorescence titration. To determine the S/N ratio, the emission intensity of RHP without Fe^{3+} was measured by 10 times and the standard deviation of blank measurements was determined. The detection limit is then calculated with the following equation:

$DL = K^* Sb_1/S$

Where K = 2 or 3 (we take 3 in this case); Sb_1 is the standard deviation of the blank solution; S is the slope of the calibration curve.

For UV-vis:

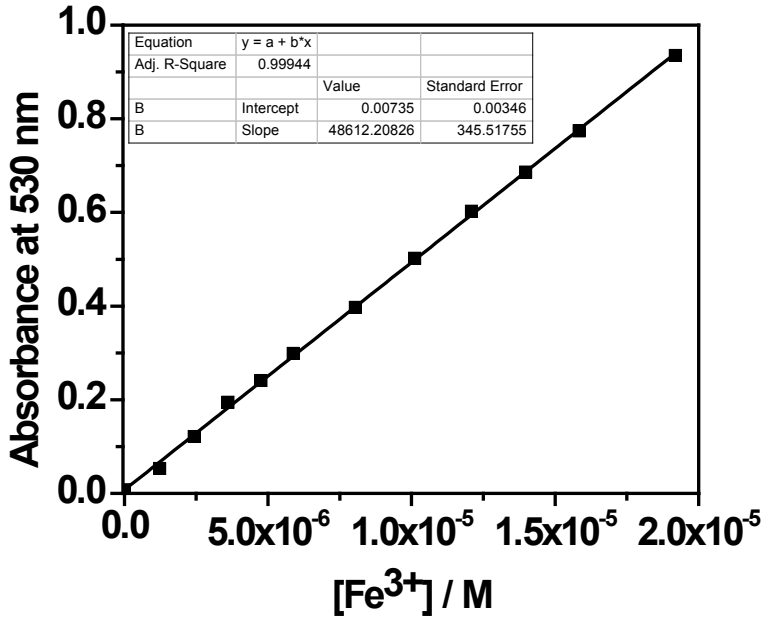

From the graph, we get slope = 48612.2082, and Sb_1 value is 0.0087

Thus using the formula we get the Detection Limit = 5.554 x 10^{-7} M i.e. RHP can detect Fe^{3+} in this minimum concentration through UV-vis method.

For Fluorescence:

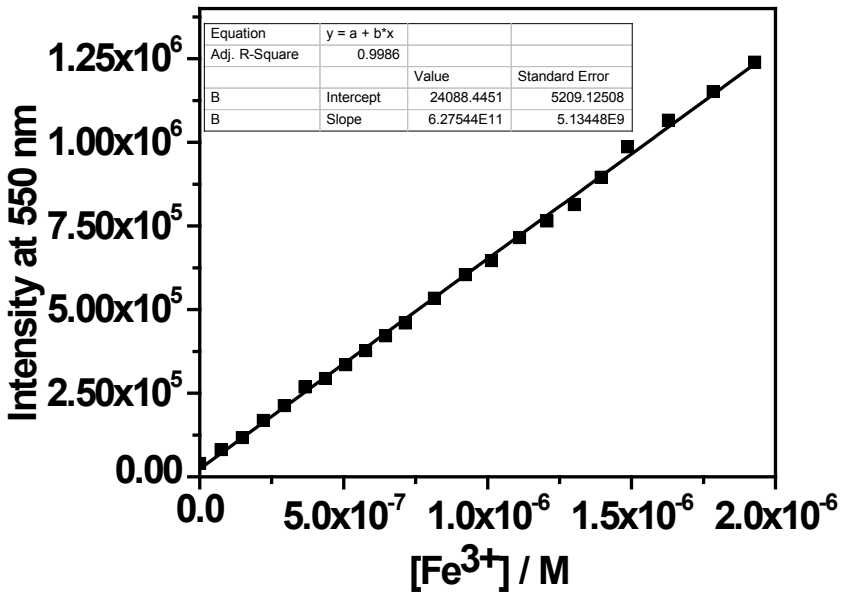

From the graph we get slope = 6.2754 x 10^{11}, and Sb_1 value is 772.76

Thus using the formula we get the Detection Limit = 3.6 x 10^{-8} M i.e. RHP can detect Fe^{3+} in this minimum concentration through fluorescence method.

ESI MS spectra of compound C:

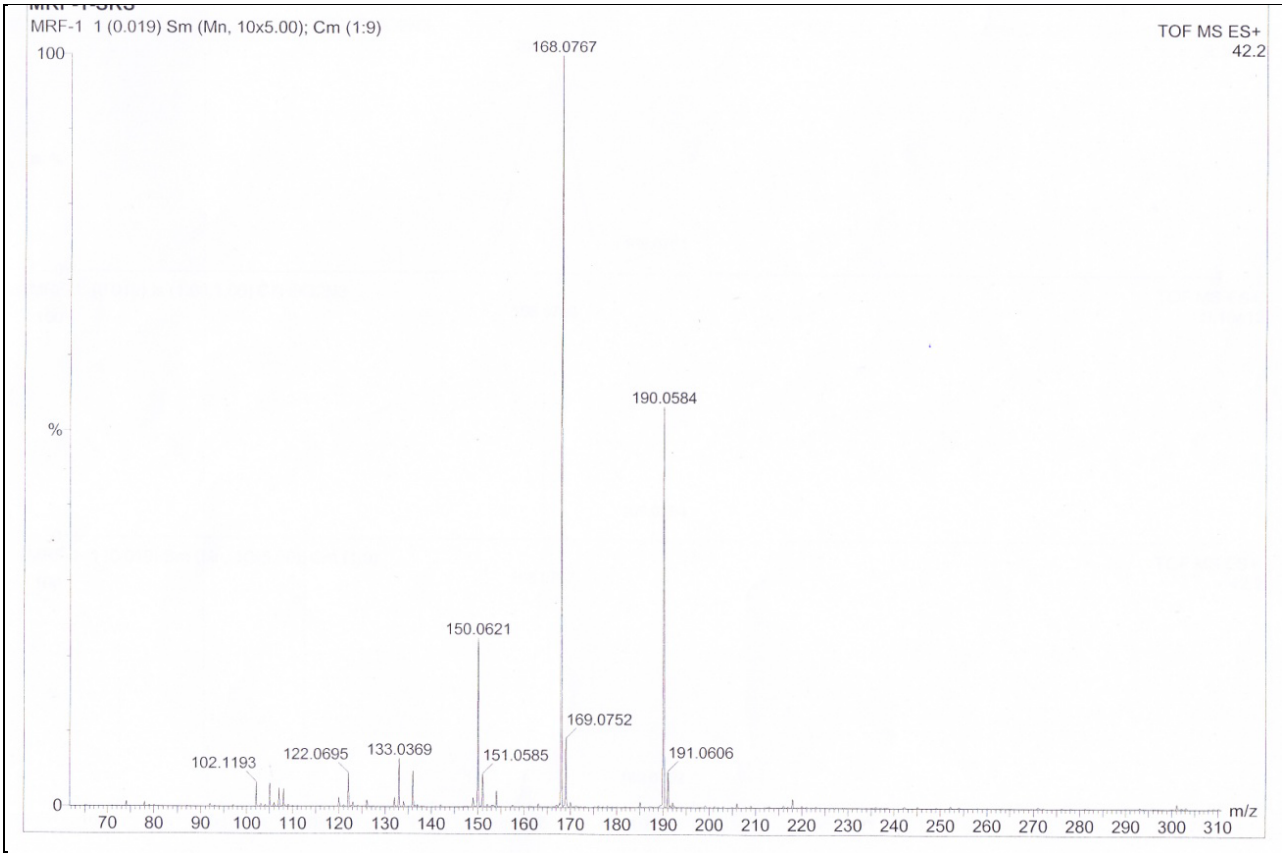

Figure S4: ESI TOF mass spectra of the compound C.

^{1} H NMR spectra of the compound C:

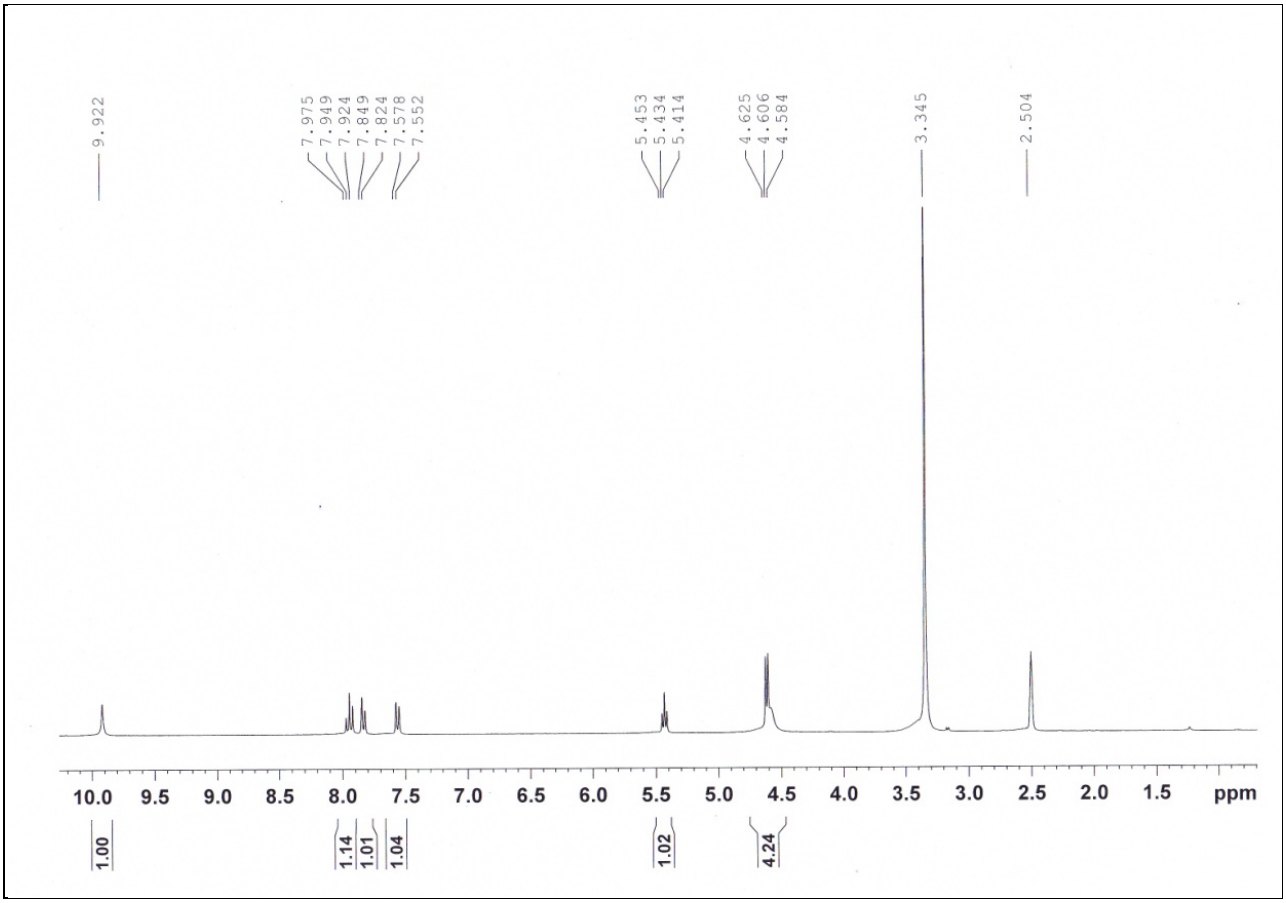

Figure S5: 1H NMR (400 MHz) spectra of compound C in d^{6} DMSO.

^{1} H NMR spectra of the receptor (RHP):

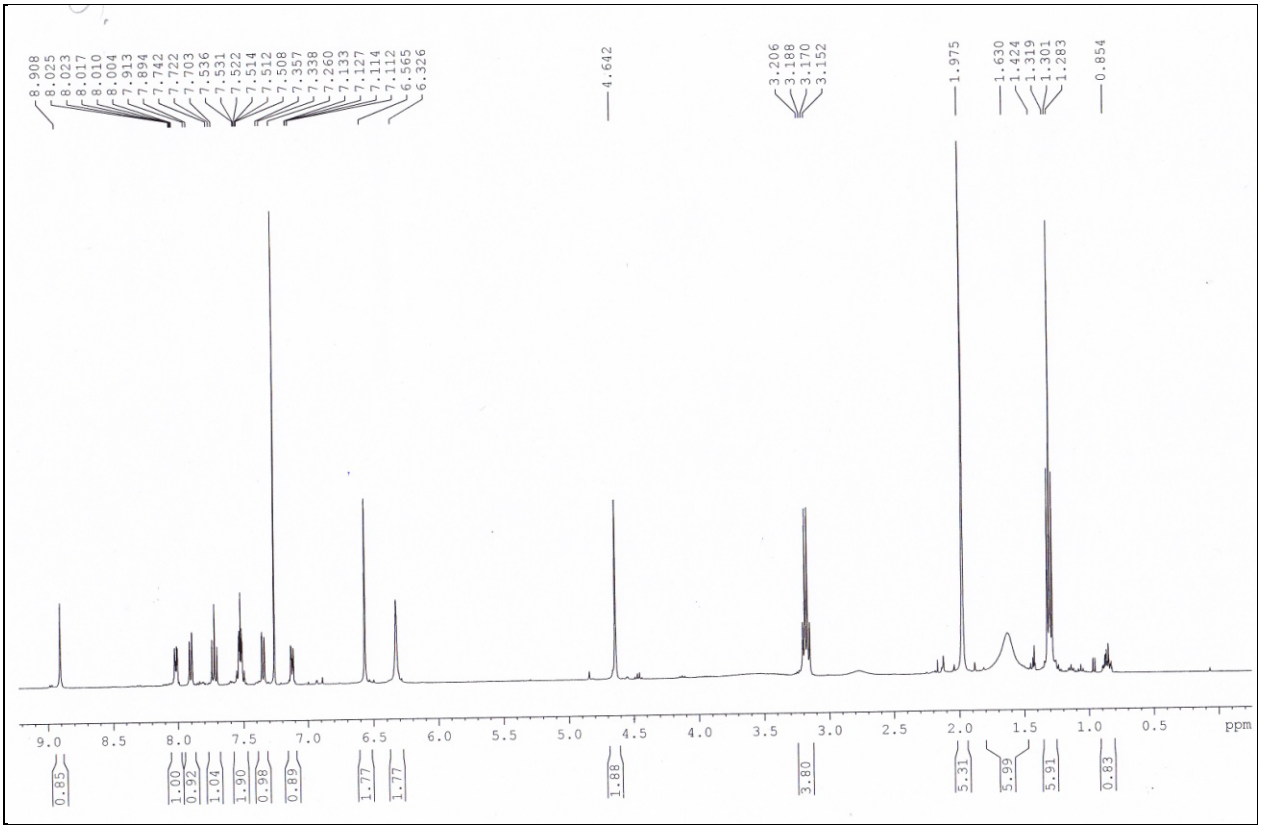

Figure S6: ^{1}H NMR (400 MHz) spectra of the receptor (RHP) in $CDCl_3$.

ESI MS spectra of the receptor:

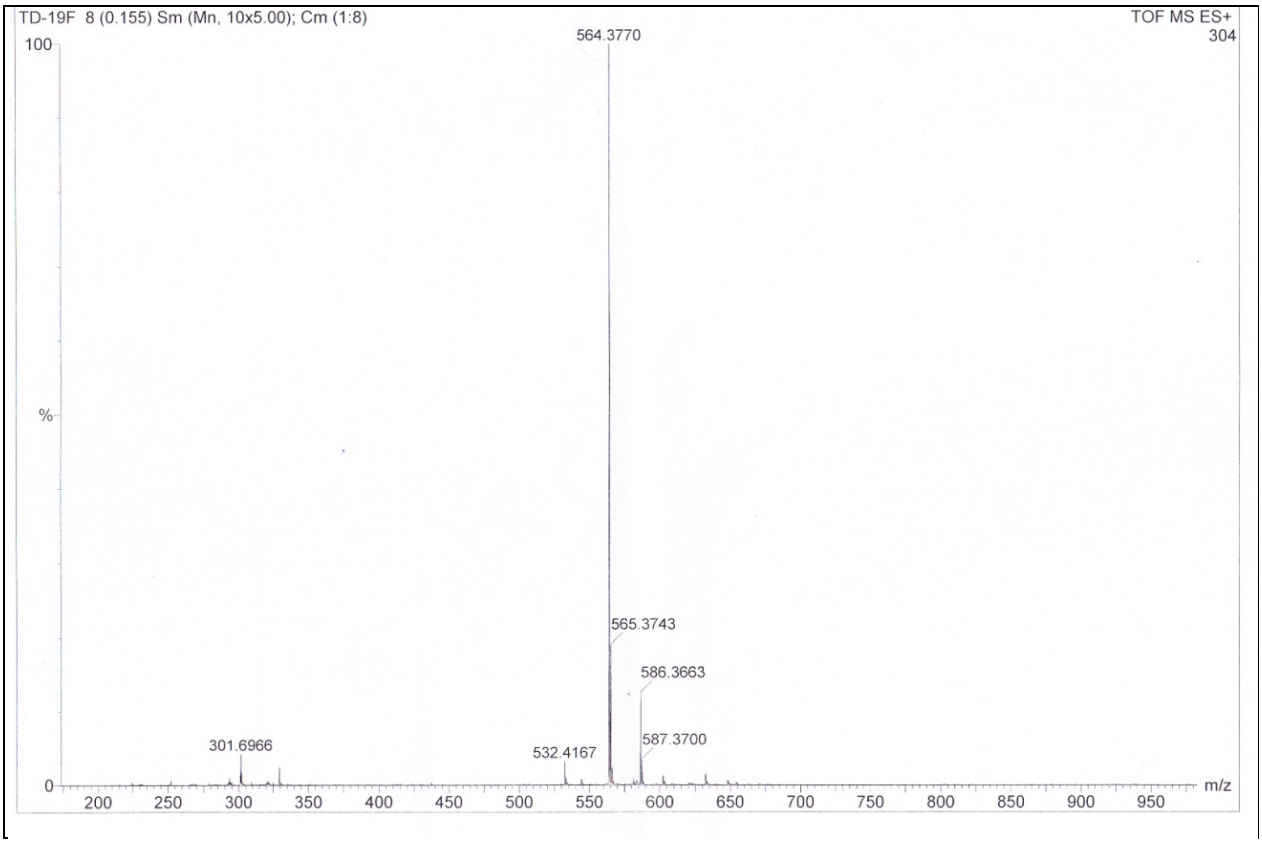

Figure S7: ESI TOF (HRMS) mass spectra of the receptor (RHP).

^{13}C NMR spectra of the receptor (RHP):

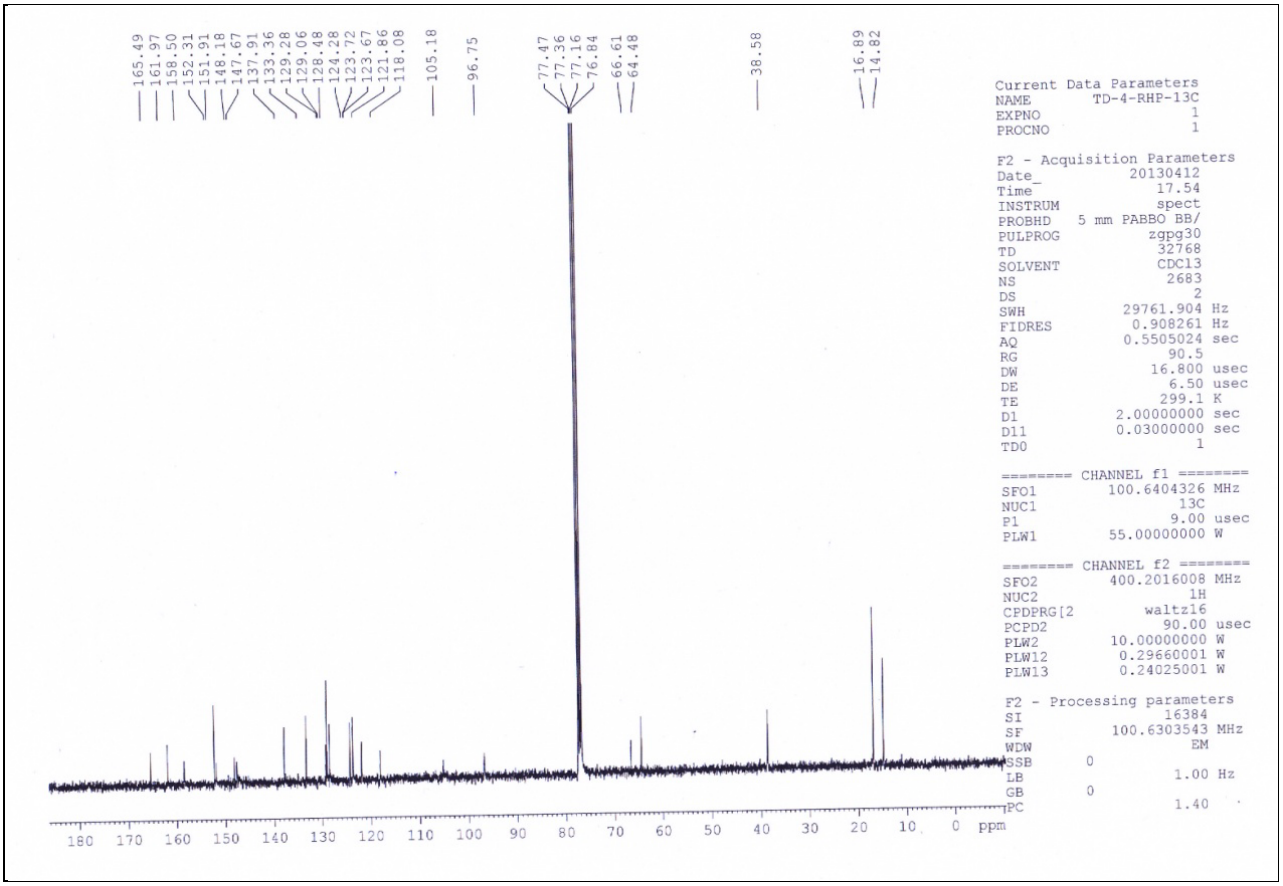

Figure S8: ^{13}C NMR (100 MHz) spectra of the receptor in $CDCl_3$.

IR spectra of the receptor and its Fe^{3+} complex:

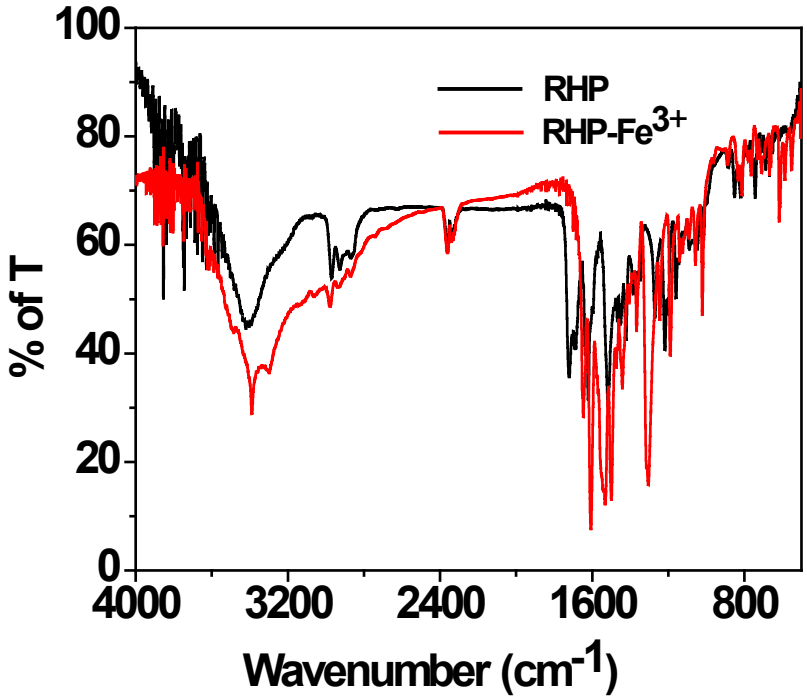

Figure S10: FT IR spectra of the receptor and its complex with Fe^{3+}.

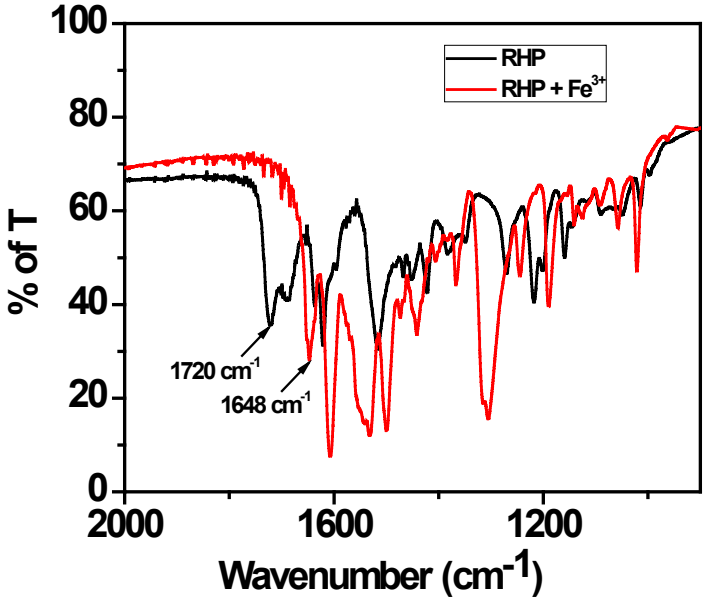

Figure S11: Partial IR spectra of RHP and its complex with Fe^{3+}

IR spectra of RHP and RHP-Fe^{3+} were taken in KBr disks, respectively. The peak at 1720 cm^{-1}, which corresponds to the characteristic amide carbonyl absorption of RHP, was shifted to 1648 cm^{-1} upon chelating with Fe^{3+}, indicating that rhodamine carbonyl group is involved in Fe^{3+} coordination.

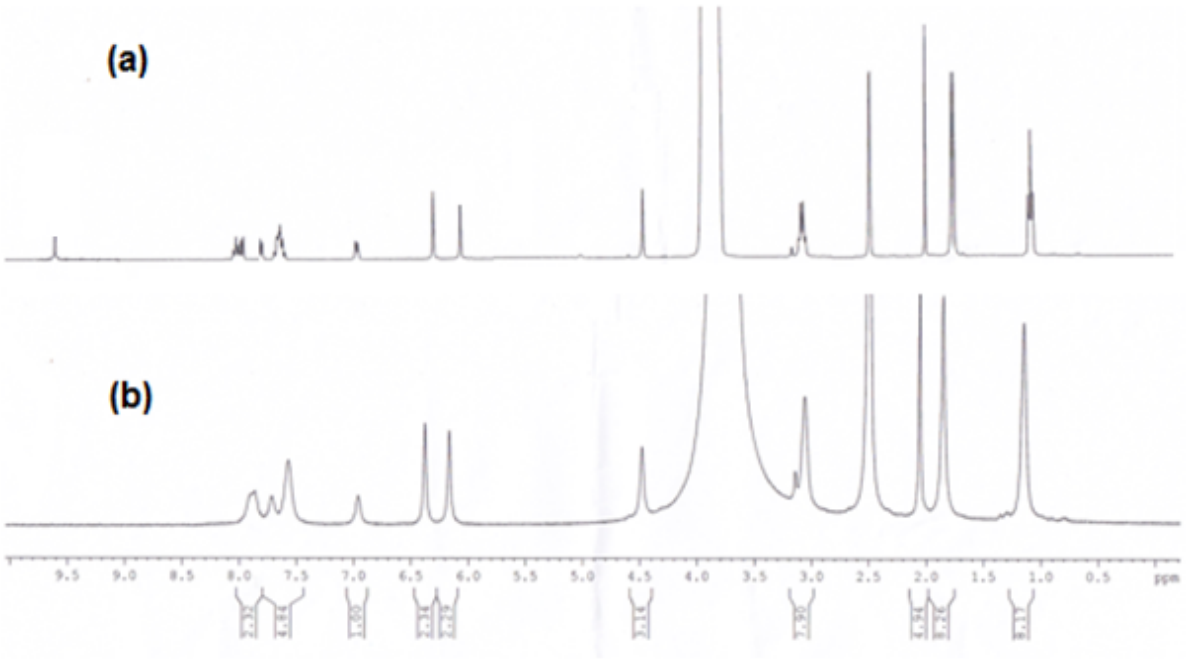

Figure S12: ^1H NMR (400 MHz) spectra of RHP (a) and its complex with Fe^{3+} (b) in d6 DMSO: D_2O (9:1).

Fluorescence emission spectra of the receptor with different guest cations in CH_3CN-HEPES buffer solution (1:1, *v/v*, pH = 7.2):

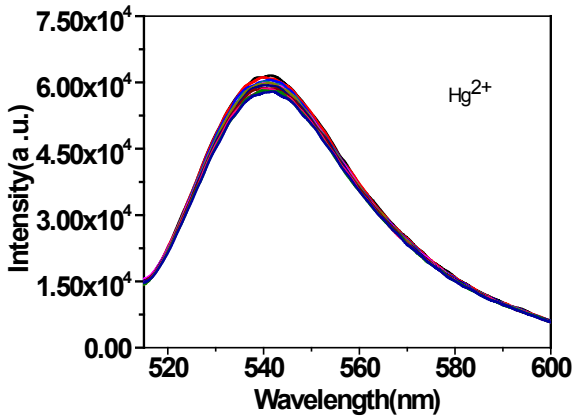

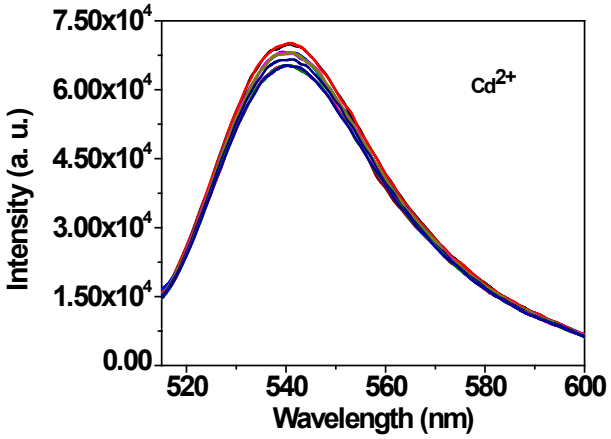

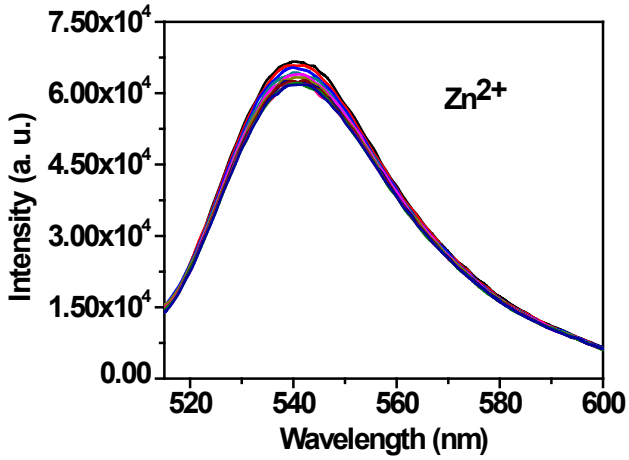

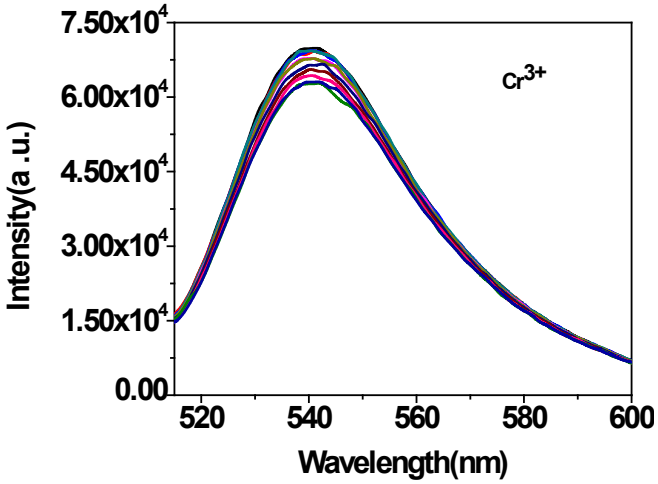

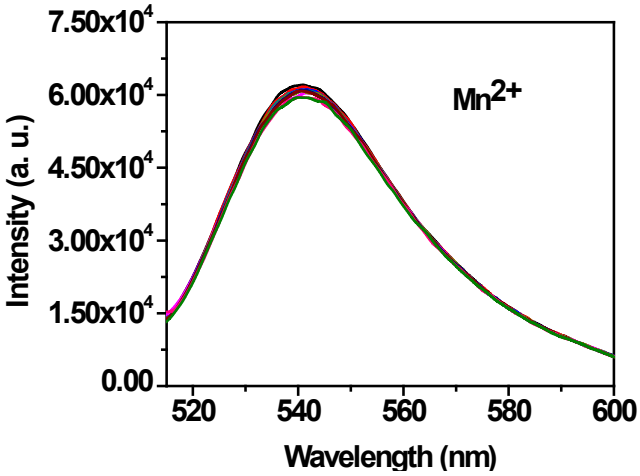

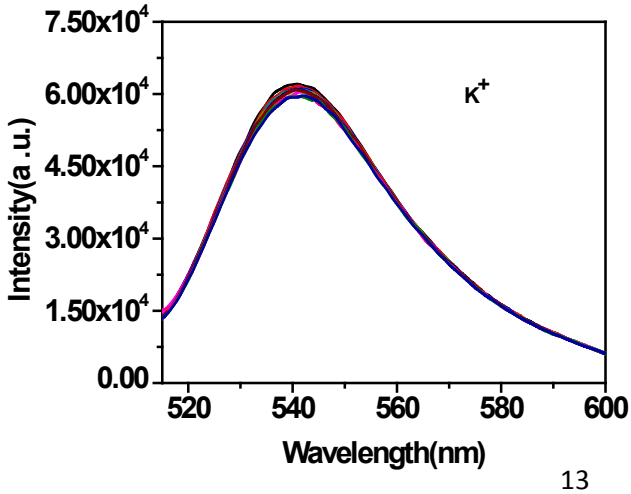

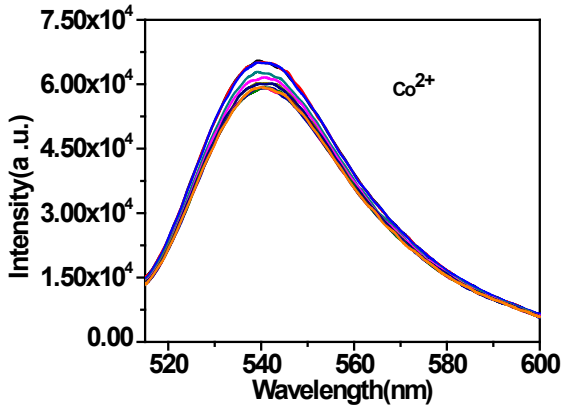

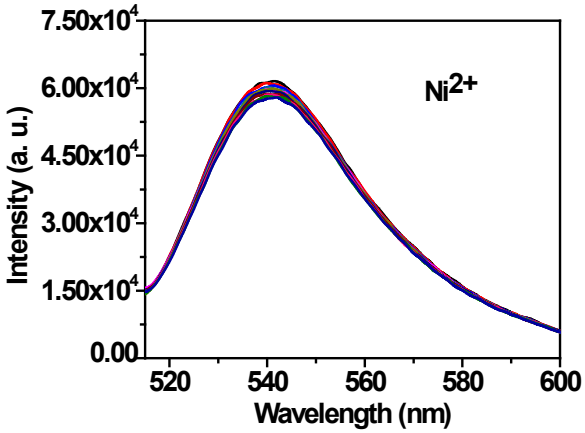

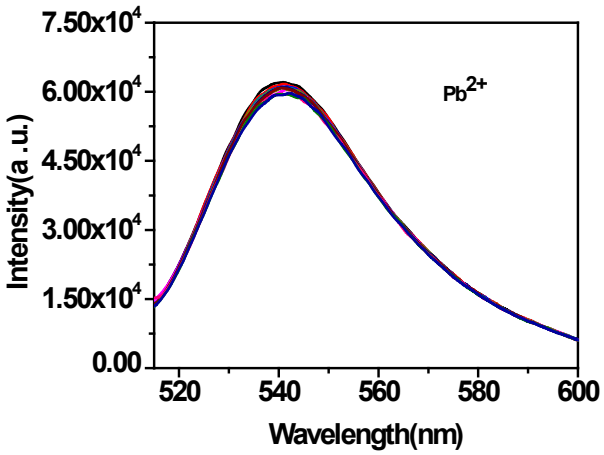

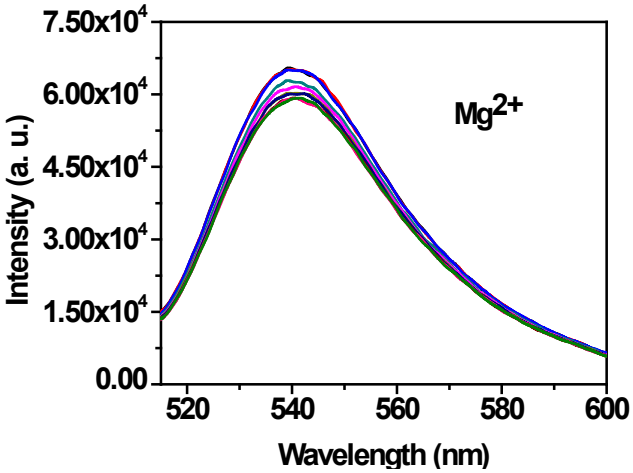

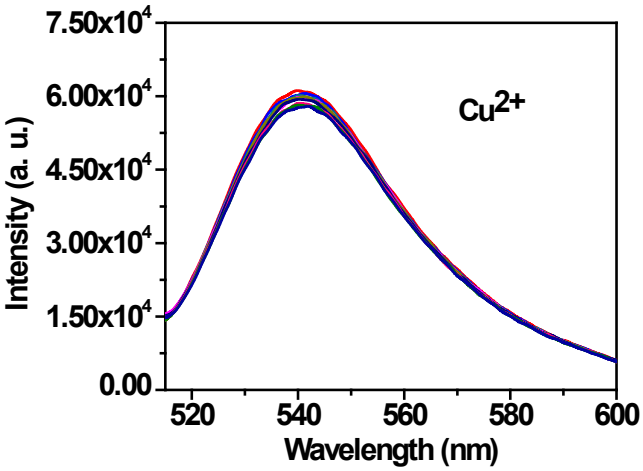

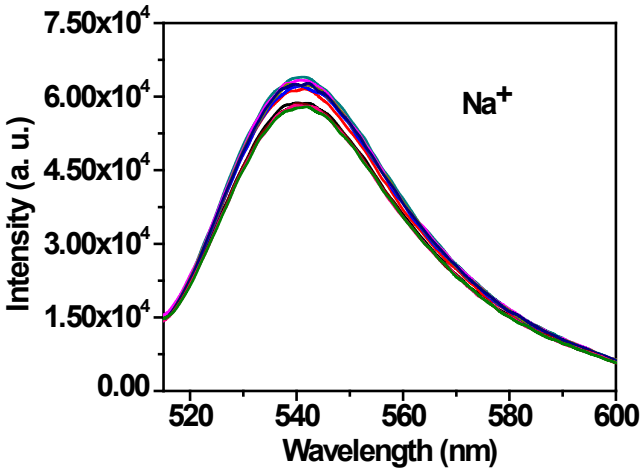

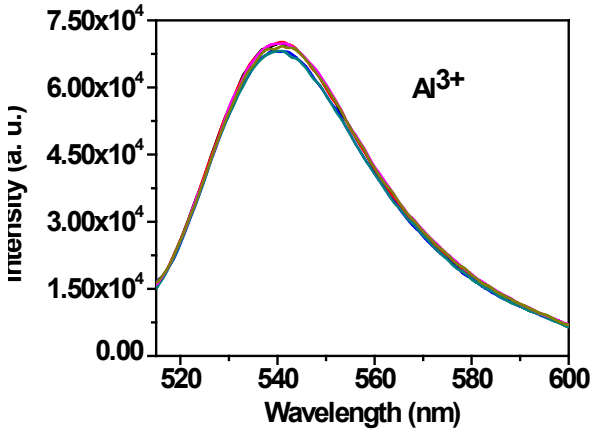

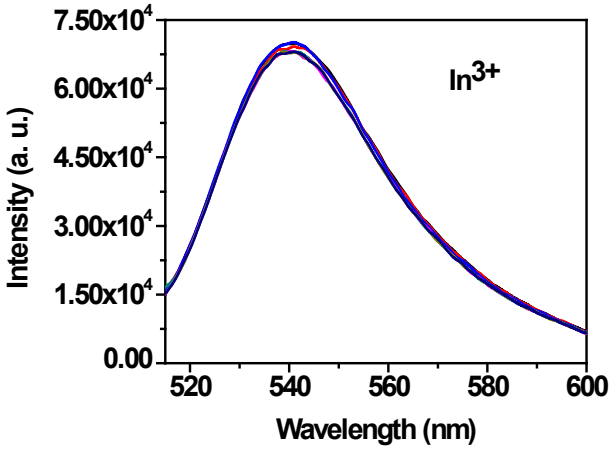

UV-vis Absorption titration spectra of the receptor with different guest cations in CH_3CN-HEPES buffer solution (1:1, *v/v*, pH= 7.2):

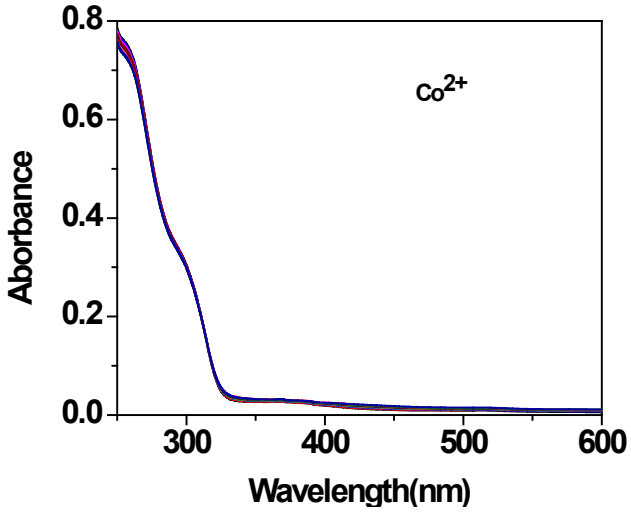

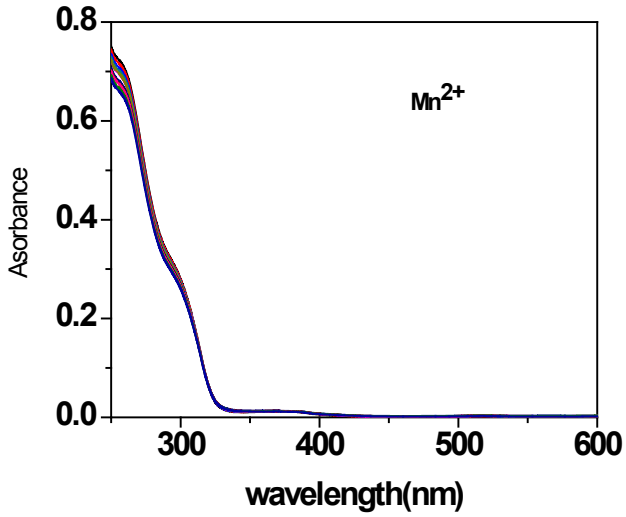

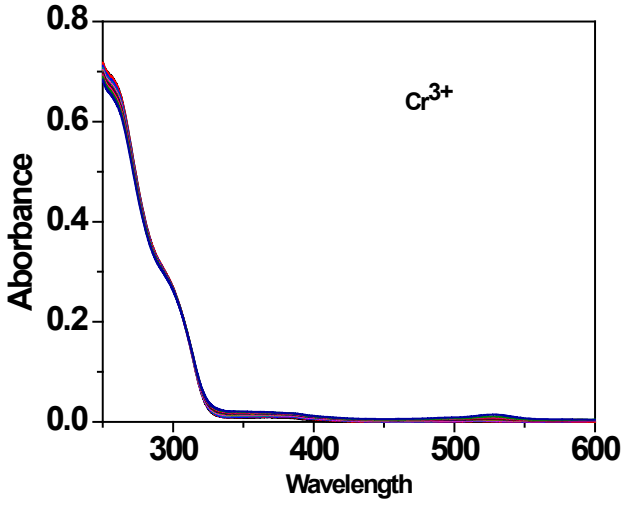

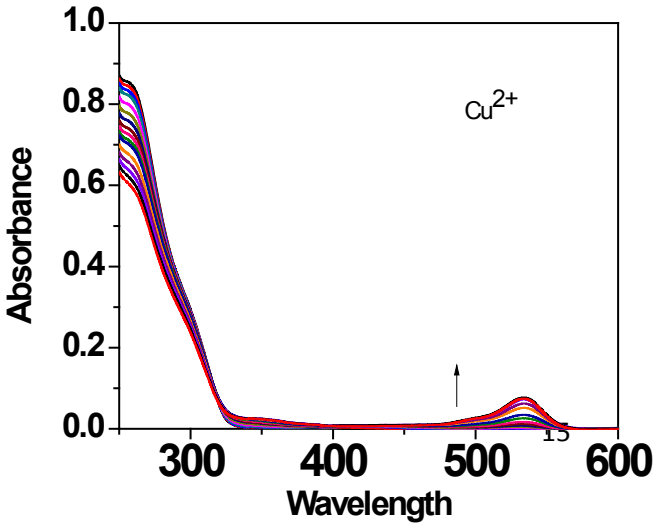

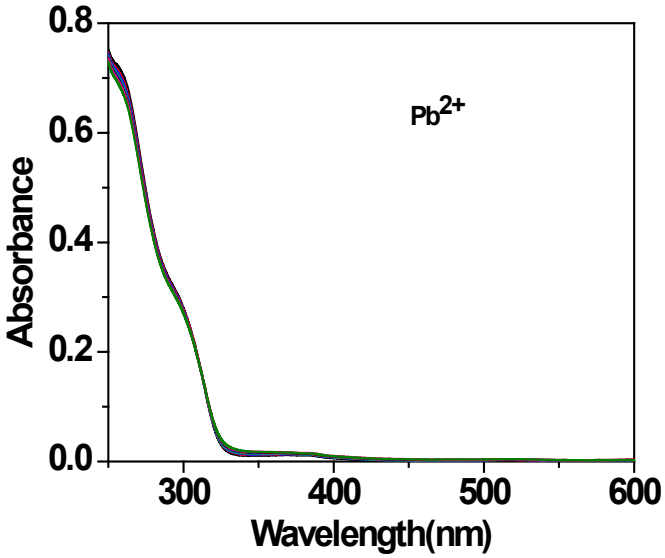

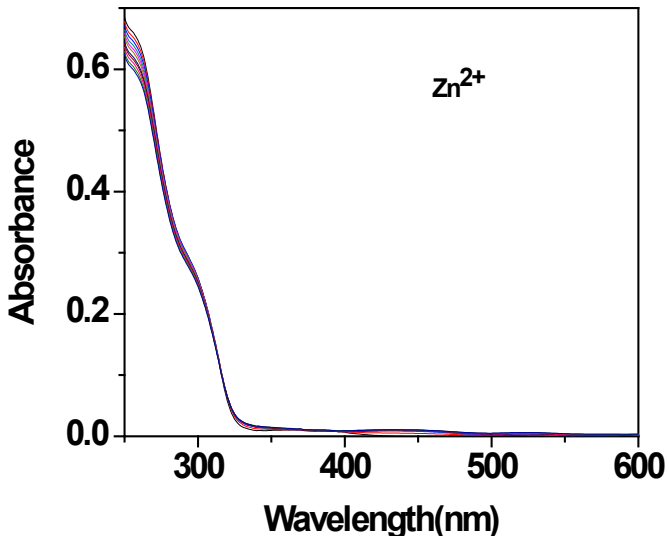

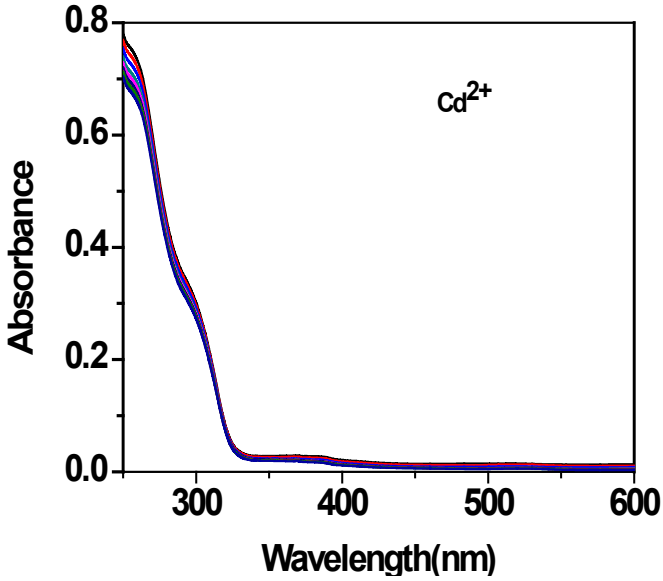

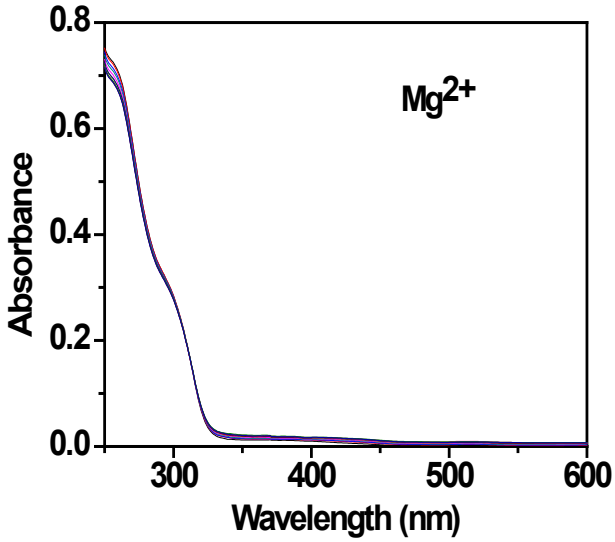

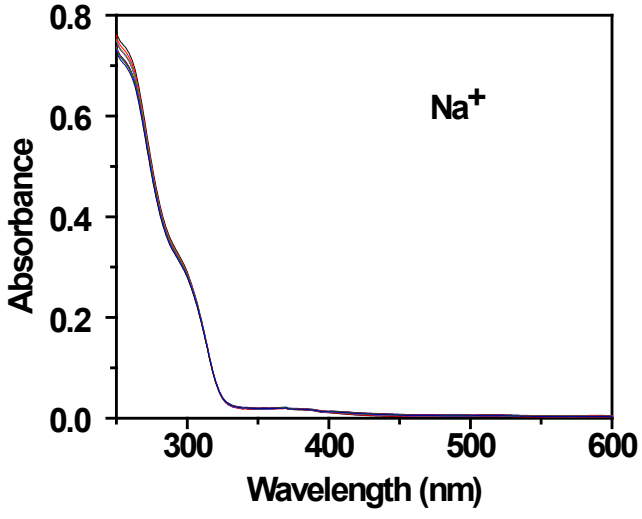

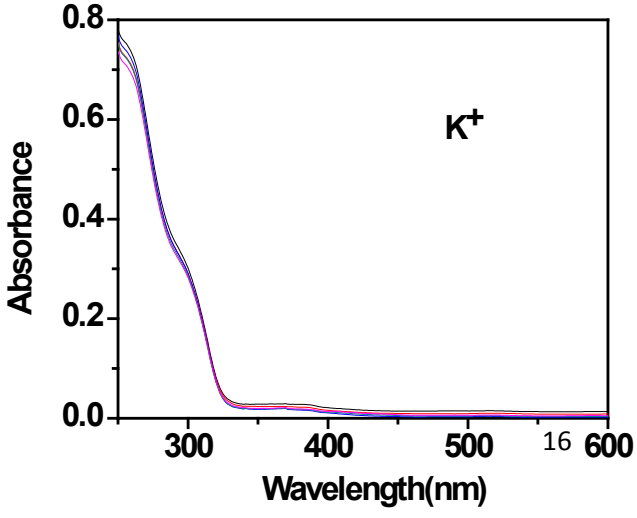

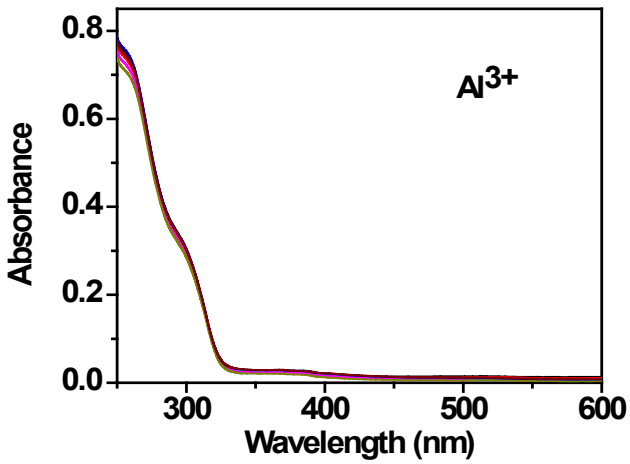

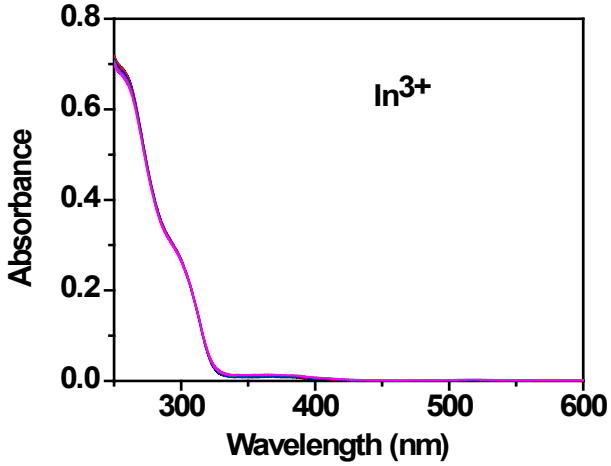

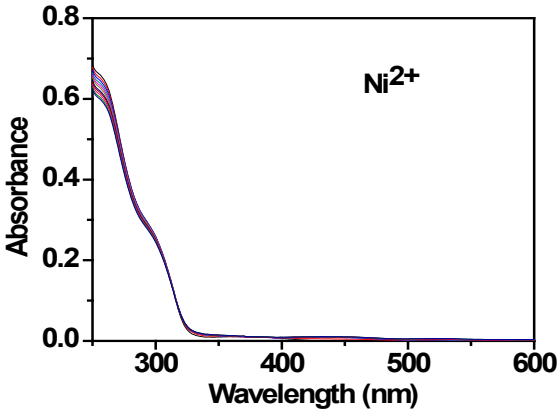

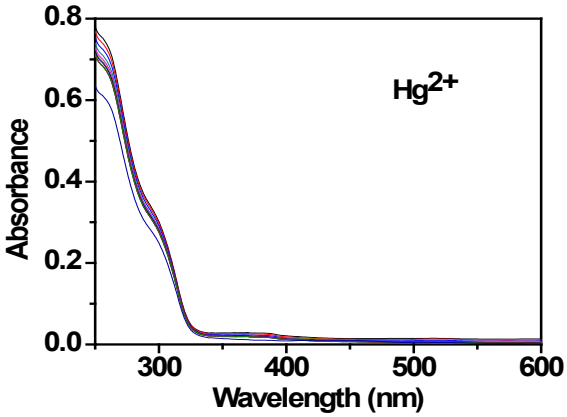

The first order rate constant was calculated from the changes of absorbance curve of RHP (20 µM) at different time interval by addition of Fe^{3+} (20 µM).

From the time vs. absorbance plot (Figure S12) at fixed wavelength 530 nm by using first order rate equation we get the rate constant = k = slope×2.303 = 3.2×10^{-2} Sec^{-1}.

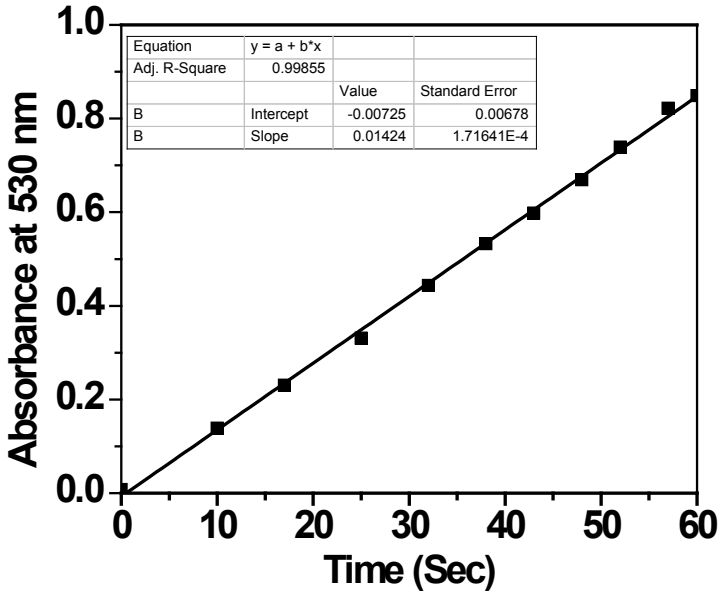

Figure S13: Time (Sec) vs. absorbance plot at 530 nm

X-ray Crystallography:

Crystal structure of the RHP was determined by single crystal X-ray diffraction from data collected at room temperature. A single crystal of 0.279 x 0.274 x 0.187 mm^3 in size was mounted on a glass fiber with epoxy cement for X-ray crystallographic study. The data were collected using a Bruker APEX2 CCD diffractometer with the graphite monochromated MoKα radiation at a detector distance of 5cm and with APEX2 software (Bruker, 2009). The collected

data were reduced using SAINT program and the empirical absorption corrections were performed using the SADABS program. The structure were solved by direct methods and refined by least-squares using the SHELXTL software package. All non-hydrogen atoms were refined anisotropically whereas hydrogen atoms were refined isotropically. All N-bound atoms were located in difference Fourier maps and refined freely. The disordered O-bound atoms were located in difference Fourier maps and refine with with U_{iso} (H) = 1.5 U_{eq} (O). The remaining hydrogen atoms were positioned geometrically with U_{iso} (H) = 1.2 or 1.5 U_{eq} (C). A rotating-group model was applied for the methyl groups.

Table 1: X-ray crystallographic data

Compounds	RHP (CCDC 935238)
Formula	$C_{33}H_{33}N_5O_4 \cdot C_2H_3N$
Formula Weight	604.70
Crystal System	Triclinic
Space Group	*P*-1
T, K	100
Z	2
a,Å	9.7783 (6)
b,Å	11.5330 (7)
c,Å	15.7730 (14)
α,deg	102.191 (2)
β,deg	95.289 (2)
γ,deg	112.724 (1)

V, Å^3	1573.63 (19)
d_{calcd} , g/cm^3	1.276
μ, mm^{-1}	0.09
Reflections with $I > 2\sigma(I)$	5662
Independent reflections	9237
θ range, deg	2.0–30.2
GOF (F^2)	1.03
R_1 (wR_2), %	0.049, 0.160

Table 2 Hydrogen-bond geometry (Å, º)

D*—H···*A	***D*—H**	**H···*A***	***D*···*A***	***D*—H···*A***
O4—H2*O*4···O3^{i}	0.87	2.28	2.931 (7)	132
C5—H5*A*···O2^{ii}	0.93	2.45	3.3328 (18)	158
C27—H27*B*···O4^{iii}	0.96	2.60	3.419 (7)	144
C30—H30*A*···O1^{iv}	0.96	2.60	3.549 (3)	171

Symmetry codes: (i) *x*+1, *y*, *z*; (ii) −*x*+1, −*y*, −*z*; (iii) *x*−1, *y*−1, *z*; (iv) −*x*+2, −*y*, −*z*+1.

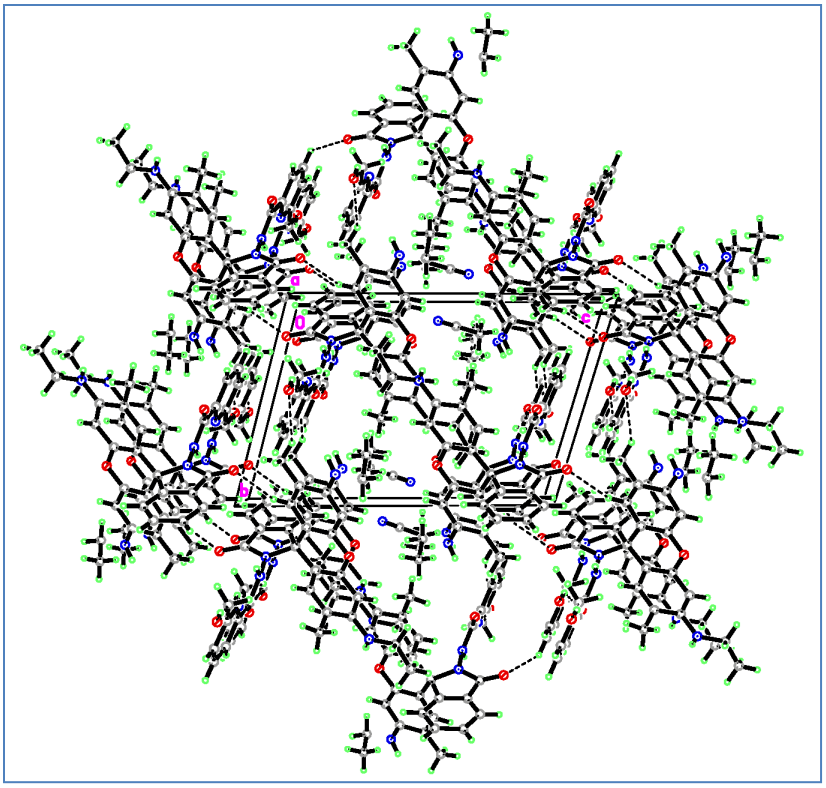

Figure S14: The molecules are linked to form a three-dimensional network

Computational study:

Computational method

Full geometry optimizations were carried out using the density functional theory (DFT) method at the B3LYP [1-3] level for the ligand RHP and its octahedral Fe^{3+} complex. All element except Fe were assigned 6-31+G(d) basis set. The LANL2DZ basis set with effective core potential (ECP) set of Hay and Wadt [4] was used for Fe. The vibrational frequency calculations were performed to ensure that the optimized geometries represent the local minima and there were only positive eigen values. Vertical electronic excitations based on B3LYP optimized geometry of RHP was computed using the time-dependent density functional theory (TDDFT) formalism [5-7] in acetonitrile using conductor-like polarizable continuum model (CPCM) [8-10]. All calculations were performed with Gaussian03 program package [11] with the aid of the GaussView visualization program.

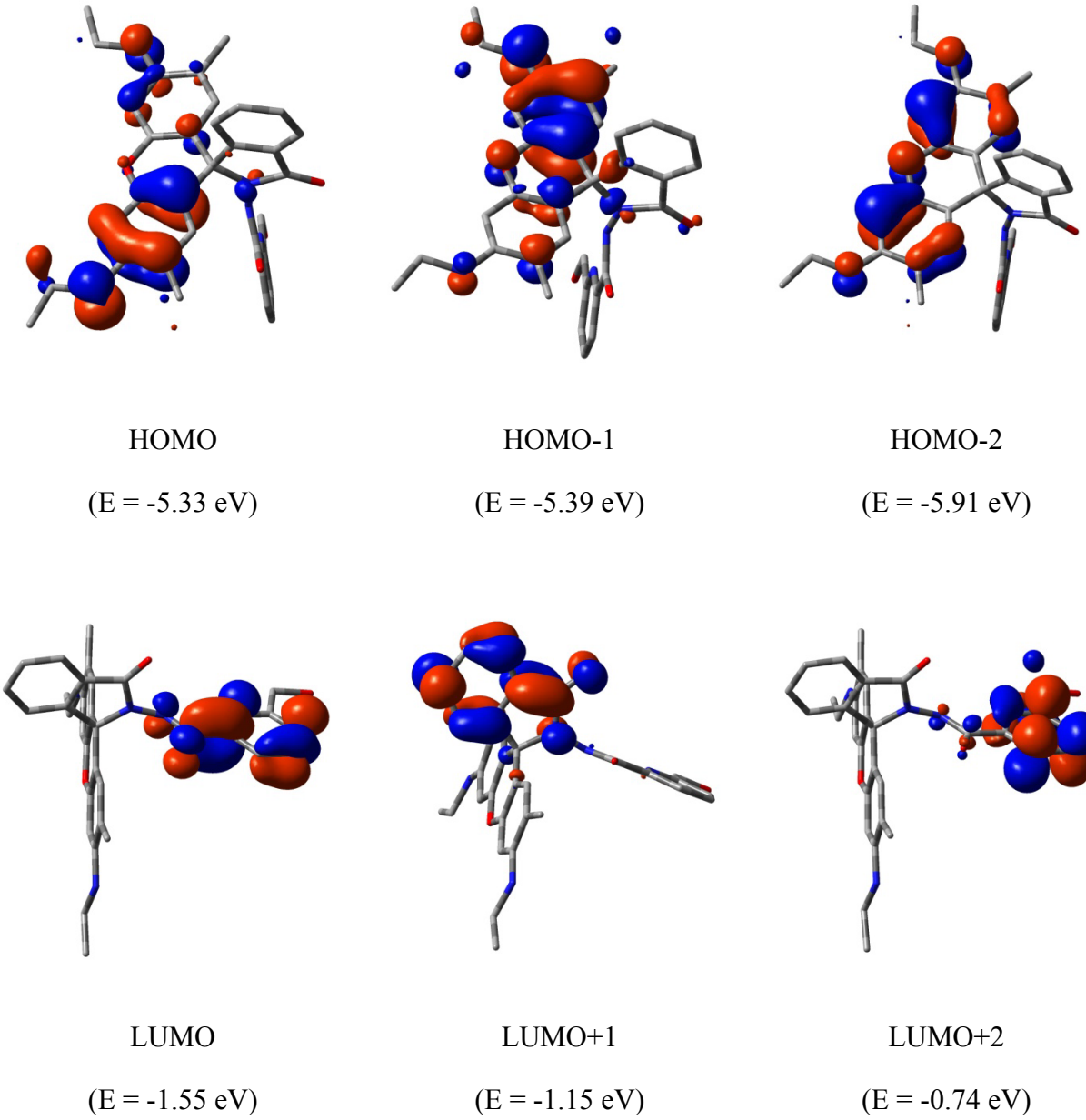

Figure S15: Contour plot of some selected molecular orbitals of RHP

Table 3 Calculated vertical electronic transitions of RHP calculated by TDDFT method

Excited state	Excitation energy (eV)	λ (nm)	Osc. Strength (f)	Key transitions
1	3.3101	374.6	0.0037	(90%)HOMO → LUMO
5	3.9068	317.4	0.0045	(85%)HOMO → LUMO+1
11	4.3103	287.7	0.0543	(76%)HOMO-1 → LUMO+3
13	4.5182	274.4	0.2060	(74%)HOMO → LUMO+4
21	4.9110	252.5	0.2984	(77%)HOMO-2 → LUMO+3

References

[1] A.D. Becke, J. Chem. Phys. 98 (1993) 5648–5652.

[2] C. Lee, W. Yang, R. G. Parr, Phys. Rev. B 37 (1988) 785–789.

[3] D. Andrae, U. Haeussermann, M. Dolg, H. Stoll and H. Preuss, Theor. Chim. Acta 77 (1990) 123–141.

[4] P. J. Hay, W. R. Wadt, J. Chem. Phys. 82 (1985) 299

[5] R. Bauernschmitt, R. Ahlrichs, Chem. Phys. Lett. 256 (1996) 454–464.

[6] R.E. Stratmann, G.E. Scuseria, M.J. Frisch, J. Chem. Phys. 109 (1998) 8218–8224.

[7] M.E. Casida, C. Jamorski, K.C. Casida, D.R. Salahub, J. Chem. Phys. 108 (1998) 4439–4449.

[8] V. Barone, M. Cossi, J. Phys. Chem. A 102 (1998) 1995–2001.

[9] M. Cossi, V. Barone, J. Chem. Phys. 115 (2001) 4708–4717.

[10] M. Cossi, N. Rega, G. Scalmani, V. Barone, J. Comput. Chem. 24 (2003) 669–681.

[11] Gaussian 03, Revision D.01, M. J. Frisch, G. W. Trucks, H. B. Schlegel, G. E. Scuseria, M. A. Robb, J. R. Cheeseman, J. A. Jr. Montgomery, T. Vreven, K. N. Kudin, J. C. Burant, J. M.

Millam, S. S. Iyengar, J. Tomasi, V. Barone, B. Mennucci, M. Cossi, G. Scalmani, N. Rega, G. A. Petersson, H. Nakatsuji, M. Hada, M. Ehara, K. Toyota, R. Fukuda, J. Hasegawa, M. Ishida, T. Nakajima, Y. Honda, O. Kitao, H. Nakai, M. Klene, X. Li, J. E. Knox, H. P. Hratchian, J. B. Cross, V. Bakken, C.Adamo, J. Jaramillo, R. Gomperts, R. E. Stratmann, O. Yazyev, A. J. Austin, R. Cammi, C. Pomelli, J. W. Ochterski, P. Y. Ayala, K. Morokuma, G. A. Voth, P. Salvador, J. J. Dannenberg, V. G. Zakrzewski, S. Dapprich, A. D. Daniels, M. C. Strain, O. Farkas, D. K. Malick, A. D. Rabuck, K. Raghavachari, J. B. Foresman, J. V. Ortiz, Q. Cui, A. G. Baboul, S. Clifford, J. Cioslowski, B. B. Stefanov, G. Liu, A. Liashenko, P. Piskorz, I. Komaromi, R. L. Martin, D. J. Fox, T. Keith, M. A. Al-Laham, C. Y. Peng, A. Nanayakkara, M. Challacombe, P. M. W. Gill, B. Johnson, W. Chen, M. W. Wong, C. Gonzalez, and J. A. Pople, Gaussian, Inc., Wallingford CT, (2004).